

BNL-108461-2015-JA

Complex Catalytic Behaviors of CuTiO_x Mixed-Oxide during CO Oxidation

Hyun You Kim^{1,2}, and Ping Liu^{2*}

¹Department of Materials Science and Engineering, Chungnam National University, 99-Daehak-ro, Yuseong-gu, Daejeon, 305-764, Korea

²Center for Functional Nanomaterials, Brookhaven National Laboratory, Upton, NY 11973, USA

Keywords: CO oxidation; CuTiO_x; Mechanism; Mixed oxide; DFT

* Corresponding author: Dr. Ping Liu

Email: pingliu3@bnl.gov

Abstract

Mixed metal oxides have attracted considerable attentions in heterogeneous catalysis due to the unique stability, reactivity and selectivity. Here, the activity and stability of CuTiO_x monolayer film supported on $\text{Cu}(111)$, $\text{CuTiO}_x/\text{Cu}(111)$, during the CO oxidation was explored using density functional theory (DFT). The unique structural frame of CuTiO_x is able to stabilize and isolate a single Cu^+ site on the terrace, which is previously proposed active for CO oxidation. However, it is not the case, where the reaction via both the Langmuir-Hinshelwood (LH) and the Mars-van Krevelen (M-vK) mechanisms are hindered on such single Cu^+ site. Upon the formation of step-edges, the synergy among $\text{Cu}^{\delta+}$ sites, TiO_x matrix and $\text{Cu}(111)$ is able to catalyze the reaction well. Depending on temperatures and partial pressure of CO and O_2 , the surface structure varies, which determines and the dominant mechanism. According to our results, the $\text{Cu}^{\delta+}$ ion that is previously proposed as active center for the CO oxidation does not work well in the form of single sites, while the synergy among multiple active sites is necessary to facilitate the reaction.

1. Introduction

Mixed metal oxides are a new class of heterogeneous catalysts which can display unique stability, reactivity and selectivity different from the individual parent oxide.¹⁻⁷ Rapid development of high-precision experimental techniques and theoretical methods in the last several decades has accelerated the rational design of multi-component oxide catalysts from fundamental insights into the chemical nature of comprising elements. Doped-oxides,⁸⁻⁹ oxide-supported-oxides,^{2-4, 10-14} or metal-supported oxides^{13, 15-17} have been reported to improve the performance of metal oxide catalysts. Different mechanisms have been proposed to pinpoint the promoting effect: (1) Each component of a mixed oxide catalyst can act as an independent reaction center to catalyze a specific elementary step involved in the overall reaction (i.e. geometric effect); (2) the electronic structure and therefore the overall catalytic activity of the oxide can be modified upon the formation of mixed oxides (i.e. electronic effect).^{8-9, 14} In addition, mixed oxides can also be employed as supports to enhance the performance of supported metal nanoparticles (NPs). It helps in controlling the particle size and the dispersion as well as maximizing the catalytic activity of metal NPs at metal-oxide interfaces via the geometric and/or electronic effects.^{2-7, 14}

Our previous study demonstrated that Cu(111) supported CuTiO_x mixed-oxide was able to stabilize the Cu⁺ ions, and CuTiO_x/Cu(111) was more active and more stable than Cu₂O(111) during CO oxidation.⁷ The cuprous oxide (Cu₂O) was reported as active catalysts for CO oxidation, where Cu⁺ ions was proposed as the critically active catalytic centers;¹⁸ however, Cu₂O catalysts underwent deactivation by either complete oxidation to CuO¹⁹ or reduction to Cu,²⁰ and therefore the lost of active Cu⁺ ions.²¹ According to our previous study, the deposition of TiO₂ clusters on Cu(111) promotes the oxidation of Cu surface and the formed TiO₂-

Cu₂O(111) interface is active toward CO oxidation. During this process, TiO₂ is reduced due to the interaction with Cu₂O(111) (electronic effect) and the reduced Ti^{δ+} with the help from Cu⁺ in the support catalyze the reaction directly (ensemble effect), being able to bind O₂ and CO well and enable a facile O-O bond cleavage via the OO-CO intermediate.¹³ However, the catalyst is not stable. TiO₂ prefers to penetrate into the substrate and form CuTiO_x monolayer film on Cu(111), CuTiO_x/Cu(111), even at 350 K.⁷

Interestingly, compared to Cu₂O(111), the formation of CuTiO_x/Cu(111) is found to display a higher CO oxidation rate, and more importantly the stability of the catalyst is significantly improved.⁷ In spite of the excellent catalytic activity and long-term stability of CuTiO_x/Cu(111) during CO oxidation, the origin of the improved performance is not well understood. On the CuTiO_x/Cu(111) surface, the Cu⁺ ions that are supposed as the active sites are separated from each other by the structural frame of TiO_x, and the synthesized CuTiO_x mixed-oxide film displays a hexagonal structural motif.⁷ Yet, the specific roles that an isolated single Cu⁺ site and the -Cu-O-Ti- interfacial sites play during the reaction remain elusive. Here, we employed density functional theory (DFT) to investigate the CO oxidation on the structural motif of model CuTiO_x/Cu(111) catalyst. According to our calculations, the enhanced activity of CuTiO_x/Cu(111) toward CO oxidation depends on the synergy among Cu⁺ ions, TiO_x matrix and Cu(111), which all contribute to the reaction via electronic and/or ensemble effects. Our results also demonstrate the importance of modeling more realistic reaction condition in providing valid mechanistic understanding of catalyst behaviors. The reaction mechanism and active centers strongly depend on the surface composition of the catalyst, which can be varied by changing the reaction conditions.

2. Computational Details

The structural model of CuTiO_x mixed-oxide was adapted from our previous work.⁷ To model CuTiO_x, a Li₂TiO₃ monoclinic crystal was optimized and Li ions were replaced with Cu. A single Ti-Cu layer with coordinating oxygen atoms was sliced and optimized on a 7×7×3 Cu(111) slab. Size of a Cu(111) slab was carefully chosen to minimize a lattice mismatch between Cu(111) and CuTiO_x. Cu and Ti ions and their interfaces of the optimized flat CuTiO_x surface and the step-edge were tested for CO oxidation. CuTiO_x step-edge was constructed by removing 1/3 of CuTiO_x layer.

We performed spin-polarized DFT calculations in a plane-wave basis with the VASP code²² and the PBE²³ functional. The interaction between the ionic core and the valence electrons was described by the projector augmented wave method,²⁴ and the valence electrons with a plane wave basis up to an energy cutoff was 400 eV. The Brillouin zone was sampled at the Γ -point due to large supercell. The convergence criteria for the electronic structure and the geometry were 10⁻⁴ eV and 0.02 eV/Å, respectively. We used the Gaussian smearing method with a finite temperature width of 0.1 eV in order to improve convergence of states near the Fermi level. Because the CuTiO_x/Cu(111) is metallic, we applied computationally less-demanding GGA-PBE rather than DFT+U scheme.²⁵ The binding energy (E_{bind}) was defined as $E_{\text{bind}} = E(\text{ads/surf}) - E(\text{ads}) - E(\text{surf})$, where E represented the total energy of the surface in interaction with an adsorbate, an adsorbate in gas-phase, and bare surface, respectively.

3. Results and Discussion

3.1 Morphology of CuTiO_x/Cu(111)

Two configurations of $\text{CuTiO}_x/\text{Cu}(111)$ were taken into considerations in our modeling. One is the terrace. Figure 1a and Figure 1b present the morphology of optimized $\text{CuTiO}_x/\text{Cu}(111)$ terrace. On the surface layer of the film, each Cu^+ ion (black, Figure 1a) is coordinated by three O^{2-} ions in the nearest neighbor and six Ti^{4+} ions in the subsurface (grey, Figure 1b). In this way, Cu^+ ions are isolated from each other, which provide the possibility for the single site catalysis. A Ti^{4+} ion is in the center of six O^{2-} ions, which is a genuine structural motif for TiO_2 crystal (light grey, Figure 1a and Figure 1b). The other configuration is the step-edge. According to our previous study of a TiO_2 cluster supported on $\text{Cu}_2\text{O}(111)$, the synergy between Cu^+ and reduced Ti^{3+} at the interface is indicated as an active center for the CO oxidation.¹³ Accordingly, to expose the $\text{CuTiO}_x\text{-Cu}(111)$ interfacial sites for the CO oxidation, we sliced off 1/3 of CuTiO_x film and constructed a step-edge (Figure 1c). During relaxation, $\text{Cu}^{\delta+}$ ions that are initially on the surface sink down and lie at step-edge (yellow, Figure 1c). Note that, the exposed $\text{Cu}^{\delta+}$ ions at the step edge are coordinated by two O^{2-} ions at the nearest neighbor, which are lower-coordinated and more reduced than Cu^+ on the terrace (ensemble effect). Accordingly to our previous studies,²⁶⁻²⁷ the reduction of $\text{Ti}^{\delta+}$ ions also takes place due to the strong interaction between $\text{Cu}(111)$ and TiO_x matrix (electronic effect). Therefore, different catalytic activities on the step edge from that on the terrace are expected.

Previously, we found that 1/3 of Cu^+ ions on the $\text{CuTiO}_x/\text{Cu}(111)$ terrace (Figure 1a) can be also stabilized in the subsurface layer;⁷ energetically this is an endothermic process, which costs 0.24 eV/ Cu^+ . Therefore, such surface configuration is not considered here for CO oxidation on the terrace of $\text{CuTiO}_x/\text{Cu}(111)$. Nevertheless, the location of Cu^+ ions on the terrace does not affect the structures of step edges. According to our calculations, both surface structures lead to

the same morphology for the step edge (Figure 1c), which is catalytically important for CO oxidation as demonstrated below.

3.2 CO oxidation on CuTiO_x/Cu(111) terrace

CO oxidation on the CuTiO_x/Cu(111) terrace starts with CO adsorption. Depending on the energetic accessibility of the oxidation pathways, CO can be directly oxidized by lattice oxygen of CuTiO_x (Mars-van Krevelen mechanism, M-vK) or oxidized by coadsorbed gas phase O₂ molecule (Langmuir-Hinshelwood mechanism, LH). Figure 2a shows that the Cu⁺ ions are the only active sites on the terrace and bind CO ($E_{\text{bind}} = -1.04$ eV) strongly at coverage of 1/12 ML. With the increasing of coverage to 1ML, CO binding is only slightly weakened ($E_{\text{bind}} = -0.93$ eV), as the active Cu⁺ sites are isolated from each other. This suggests that each Cu⁺ ion might acts as an independent active center and the catalysis should be spatially localized. However, the isolation of active Cu⁺ sites also prevents the adsorption of O₂ due to the lack of high symmetric Cu⁺ sites ($E_{\text{bind}} = 0.20$ eV). As a result, the only accessible CO oxidation pathway is via the M-vK mechanism. That is, the CO adsorbed (*CO) on the Cu⁺ site of CuTiO_x/Cu(111) terrace reduces the surface by removing the nearby surface O and produce CO₂. Figure S1 presents the formation energy of oxygen vacancy, E_{form} , via the O-CO type reaction intermediate and the corresponding activation energy, E_{b} . Upon the formation of the O-CO type intermediate, the Cu⁺ ion is shifted from the original three-fold site, which losses one of three Cu-O bonds and decreases the coordination number to two. The calculated E_{form} is -0.17 eV. Thus, the formation of oxygen vacancy next to the active Cu⁺ site is thermodynamically favorable; however, kinetically it is effectively prevented by the extremely high E_{b} of 2.62 eV. In

comparison with $\text{Cu}_x\text{O}/\text{Cu}(111)$,²⁸ $\text{CuTiO}_x/\text{Cu}(111)$ is much more stable and more difficult to be reduced or oxidized under the CO oxidation condition. That is, the formation of CuTiO_x mixed oxide provides a framework of TiO_2 to stabilize Cu_xO by hindering the reduction of the oxide during the CO oxidation. Therefore, the M-vK mechanism is also not feasible for the CO oxidation on $\text{CuTiO}_x/\text{Cu}(111)$. Given that, the experimentally observed activity toward CO oxidation⁷ is not contributed from the $\text{CuTiO}_x/\text{Cu}(111)$ terrace. The reaction via the LH mechanism is prevented due to the selective adsorption Cu^+ sites to CO rather than O_2 , while that via the M-vK mechanism is hindered due to the high stability of the mixed oxide.

3.2.1 CO oxidation on CuTiO_x step-edge

To explain the experimentally observed activity of $\text{CuTiO}_x/\text{Cu}(111)$ toward CO oxidation, we now move from the inactive terrace to the step-edge. Figure 2b shows that similar to the case of terrace, the $\text{Cu}^{\delta+}$ ion is also isolated at the step edge and strongly binds CO ($E_{\text{bind}} = -1.49$ eV). However, different behaviors are observed for O_2 adsorption. At the step edge, the reduced $\text{Ti}^{\delta+}$ sites are also available for the reaction. Both $\text{Ti}^{\delta+}-\text{Ti}^{\delta+}$ ($E_{\text{bind}} = -1.49$ eV) and $\text{Ti}^{\delta+}-\text{Cu}^{\delta+}$ ($E_{\text{bind}} = -1.60$ eV) bridge sites are able to readily stabilize adsorbed O_2 ($^*\text{O}_2$), where the adsorption at the $\text{Ti}^{\delta+}-\text{Cu}^{\delta+}$ site leads to an easy dissociation into two O atoms ($E_b = 0.28$ eV, Figure 2c and Figure 2d). Such enhanced adsorption for O_2 at the $\text{Cu}^{\delta+}-\text{Ti}^{\delta+}$ site is consistent with our previous finding observed in the $\text{TiO}_2/\text{CuO}_2(111)$ system.¹³ Accordingly, CO and O_2 adsorptions are likely to compete for the active $\text{Cu}^{\delta+}$ sites at the $\text{CuTiO}_x/\text{Cu}(111)$ step edge. To quantify that, we calculated the temperature-dependent of the adsorbed CO ($^*\text{CO}$) and O_2 ($^*\text{O}_2$) coverage at the step edge on the basis of a simplified kinetic model (Figure 3, see supporting

information for details). Under the oxygen-rich CO oxidation condition ($p_{O_2}=157$ torr, $p_{CO}=8$ torr, $T=300K$),²⁹ most of the Cu sites are occupied by $*O_2$ bound to the $Cu^{\delta+}-Ti^{\delta+}$ interface and the coverage of CO at the $Cu^{\delta+}$ site is marginal (max. 1.6 % at 620 K, Figure 3a). However, under the CO-rich condition applied for the demonstration of the $CuTiO_x$ catalyst in our previous report ($p_{O_2}=10$ torr, $p_{CO}=20$ torr, $T=300K$),⁷ the coverage of $*CO$ increases as a function of temperature, which reaches to maximum, 36 %, at 580 K (Figure 3b). Given that, the coverage of $*CO$ and $*O_2$ at the step edge can be varied by changing the temperatures and/or the p_{CO}/p_{O_2} ratios. In fact, our calculations show that such relationship is also valid at variety of p_{CO}/p_{O_2} ratios. One can see in Figure 3c and Figure 3d that at a certain p_{CO}/p_{O_2} ratio, the $*CO$ coverage increases with the temperature increasing from 300 K to 500 K. However, both $*CO$ and $*O_2$ become unstable as temperature is further increased, and eventually desorb from the step edge. Of course, by comparing Figure 3a and Figure 3b, one can see that increasing the pressures of CO and O_2 is able to hinder the desorption to some extent; yet the optimal catalytic activity is likely to be achieved below 600 K as both $*CO$ and $*O_2$ can be stabilized at the step edge and readily for the CO oxidation reaction. That is, during the CO oxidation reaction below 600K the $Cu^{\delta+}$ sites can be occupied by either $*O_2$ or $*CO$. Accordingly, for our mechanistic study we considered the CO oxidation on both O_2 -adsorbed and CO-adsorbed $CuTiO_x/Cu(111)$ step edges. We note that the effect of temperature/partial pressure on the CO and O_2 coverage is only considered for the step edge, rather the terrace, where the O_2 adsorption cannot compete with the CO adsorption and the terrace Cu ions are dominantly covered with CO.

3.2.2 O_2 -adsorbed $CuTiO_x/Cu(111)$ step-edge

As presented in Figure 2d, at the CuTiO_x/Cu(111) step edge the strong interaction between O₂ and the Cu^{δ+}-Ti^{δ+} site allows a facile dissociation with a low E_b of 0.28 eV. Thus the oxidation of the step-edge is likely to occur under the reaction conditions, which is not the case on the terrace (Figure 4, S1, S2). That is, the step edge of CuTiO_x/Cu(111) is more oxophilic than the terrace and can be significantly stabilized by oxidation. Accordingly, the LH pathway rather than the M-vK is more likely for the CO oxidation at the CuTiO_x/Cu(111) step edge. After the *O₂ dissociation, the Cu^{δ+} ion can still bind CO with E_{bind} of -0.86 eV (Figure 4a, S3). The first CO₂ production (Figure 4a, S3, S4) is favorable both thermodynamically ($E_{\text{form}} = -1.62$ eV) and kinetically ($E_b = 0.42$ eV). The produced CO₂ can be easily removed ($E_{\text{des}} = -0.02$ eV) and the remaining *O stays at the Cu^{δ+}-Ti^{δ+} site.

Oxidation of the first *CO at the Cu^{δ+} site of step-edge is facile and energetically. The energy released after the reaction has reached the heat of reaction for the oxidation of two CO molecules in gas phase (Figure 4a, dashed line). Oxidation of the second *CO is problematic (Figure 4a). The second CO is still able to interact well with the Cu^{δ+} site ($E_{\text{bind}} = -0.94$ eV, S6). The reaction by combining *CO and the remaining *O from O₂ dissociation at the Cu^{δ+}-Ti^{δ+} site to produce *CO₂ is almost thermoneutral ($E_{\text{form}} = 0.06$ eV); yet the barrier is not high ($E_b = 0.42$ eV). It is the *CO₂ desorption from the step-edge, which is highly endothermic and likely slows down the overall reaction ($E_{\text{des}} = 1.04$ eV, S7). Both S6 and S7 states are under the theoretical total reaction energy line, which results in a deep energy well and the slowdown of the overall conversion. A large portion of such high E_{des} of CO₂ comes from the energy cost to recover the distorted step-edge by interacting with the adsorbates, which also indicates the low stability for the local structures of the step-edge. Interestingly, we find that the oxidation of the second *CO by an additional O₂ adsorbed at the Cu^{δ+}-Ti^{δ+} site ($E_{\text{bind}} = -0.99$ eV) (Figure 4b, S7') can facilitate

the overall CO oxidation. In this case, *CO reacts with *O₂ to produce *CO₂ is more exothermic ($E_{\text{form}} = -2.56$ eV) than that with the existing *O ($E_{\text{form}} = 0.06$ eV) due to the high oxophilic feature of the step-edge; yet by involving the O-O cleavage the corresponding barrier for *CO oxidation by *O₂ is slightly higher ($E_b = 0.50$ eV, Figure 4b, S8') than that by *O ($E_b = 0.42$ eV). The big difference is observed for *CO₂. Involving the additional oxygen leads to the surface oxidation (Figure 4b). As a result, the CO₂ binding is weakened and the bottleneck *CO₂ desorption (Figure 4a) is promoted, where the energy cost for removing *CO₂ ($E_{\text{des}} = 0.47$ eV) is lowered down to only 46 % of that in the previous case (Figure 4a). At the final stage (Figure 4b, S9), the *O removed by the first *CO is recovered and the morphology of the step edge returns back to S2. Therefore, O₂-adsorbed CuTiO_x/Cu(111) step-edge is not stable under the CO oxidation condition, but likely to get oxidized; in comparison, the oxidized CuTiO_x/Cu(111) step-edge is more stable and more active toward CO oxidation via the LH mechanism, being able to bond CO and O₂ well, but still allowing the facile CO₂ formation and removal. Given that, the oxidized step-edge is a catalytic reaction center for the CO oxidation on the O₂-adsorbed CuTiO_x/Cu(111) step edge. Therefore, under the CO oxidation, the oxidation of *CO by *O₂ is likely to dominate rather than that by *O, when both oxidizing agents are available at the step-edge. The facilitated CO oxidation is attributed to the surface oxidation resulted from the additional oxygen, which promotes the bottleneck *CO₂ desorption and therefore the overall CO oxidation.

3.2.3 CO-adsorbed CuTiO_x/Cu(111) step-edge

Although the thermodynamics shows a large portion of the $\text{Cu}^{\delta+}$ sites at the $\text{CuTiO}_x/\text{Cu}(111)$ step-edge covered by $^*\text{O}_2$ rather than $^*\text{CO}$, the amount of $^*\text{CO}$ can be increased and become significant with the increasing $p_{\text{CO}}/p_{\text{O}_2}$ ratio and temperature (Figure 3). As CO binds to the on-top site of $\text{Cu}^{\delta+}$ ($E_{\text{bind}} = -1.49$ eV, Figure 5a, S1), the $\text{Ti}^{\delta+}$ - $\text{Ti}^{\delta+}$ bridge site is still available for O_2 coadsorption ($E_{\text{bind}} = -1.20$ eV, Figure 5a, S2). Although such $^*\text{O}_2$ is not as strong as that at the $\text{Cu}^{\delta+}$ - $\text{Ti}^{\delta+}$ sites (Figure 2), it is active enough to oxidize the nearby $^*\text{CO}$ via the LH mechanism. The reaction is highly exothermic with almost no barrier ($E_{\text{form}} = -3.06$ eV, $E_{\text{b}} = 0.01$ eV, Figure 5a, S3), and the produced $^*\text{CO}_2$ can be easily removed ($E_{\text{des}} = 0.09$ eV, Figure 5a, S4). Such strong driving force of $^*\text{CO}_2$ formation again confirms the appropriate oxophilic nature of the step edge, which enables both facile CO_2 formation and desorption. After oxidization of the first CO, we tested two different binding sites for the second CO: $\text{Cu}^{\delta+}$ at the step edge (yellow) and $\text{Cu}^{\delta+}$ on the terrace (black). In both cases, $\text{Cu}^{\delta+}$ strongly binds CO molecule ($E_{\text{bind}} = -1.41$ vs. -1.11 eV, Figure 5a, S5) and the $^*\text{CO}_2$ formation is activated both thermodynamically ($E_{\text{form}} = 0.48$ vs. 0.25 eV, Figure 5a, S6) and kinetically ($E_{\text{b}} = 1.07$ vs. 1.25 eV), though removal of $^*\text{CO}_2$ should be fairly fast ($E_{\text{des}} = 0.06$ vs. -0.01 eV, Figure 5a, S7). Given that, the LH mechanism is not likely at the CO-adsorbed $\text{CuTiO}_x/\text{Cu}(111)$ step edge.

The other possible pathway for CO oxidation is via the general M-vK mechanism. The first $^*\text{CO}$ is oxidized by adjacent lattice oxygen to form $^*\text{CO}_2$ (Figure 5b, S2). This is an exothermic step ($E_{\text{form}} = -0.61$ eV) with no barrier ($E_{\text{b}} = 0.03$ eV). Upon the facile $^*\text{CO}_2$ desorption ($E_{\text{des}} = 0.44$ eV, Figure 5b, S3), an oxygen vacancy is formed, which provides an active site for O_2 adsorption ($E_{\text{bind}} = -1.84$ eV, Figure 5b, S4). $^*\text{O}_2$ not only fills the oxygen vacancy, but also readily reacts with the second $^*\text{CO}$ adsorbed at the $\text{Cu}^{\delta+}$ site next to $^*\text{O}_2$ ($E_{\text{bind}} = -1.11$ eV, Figure 5b, S5) to form $^*\text{CO}_2$. The reaction is energetically favorable ($E_{\text{bind}} = -1.98$

eV, $E_b \leq 0.01$ eV, Figure 5b, S6) and the produced *CO_2 can be removed efficiently ($E_{des} = 0.06$ eV, Figure 5b, S7). The low activation energy barriers and the smooth reaction diagram (without a high bump and a deep potential well) assure the feasibility of the M-vK type of CO oxidation mechanism at the CO-adsorbed $CuTiO_x/Cu(111)$ step-edge.

4. Discussion

According to our mechanistic study using DFT, the activity of $CuTiO_x/Cu(111)$ model catalyst toward CO oxidation observed experimentally is contributed from the step-edge, rather than the terrace. The unique structural frame of $CuTiO_x$ mixed-oxide supported on $Cu(111)$ generates a unique isolated single $Cu^{\delta+}$ site on both the terrace and the step-edge of $CuTiO_x/Cu(111)$. Cu^+ is the only active centers during CO oxidation on the terrace, being only selective for adsorbing CO, rather than O_2 due to the lack of high symmetric sites constructed by Cu^+ . As a result, the LH mechanism is prohibited. The M-vK mechanism is also not feasible due to the highly stable oxygen on the surface achieved by the formation of $CuTiO_x$ mixed oxide.

Upon the formation of step-edges, two different active sites are available for CO oxidation: $Cu^{\delta+}$ and $Ti^{\delta+}$. Both $Cu^{\delta+}-Ti^{\delta+}$ and $Ti^{\delta+}-Ti^{\delta+}$ bridge sites are able to stabilize O_2 and break O-O bond efficiently during CO oxidation, while $Cu^{\delta+}$ still maintains its strong CO binding. Under the O_2 -rich conditions, the active sites at the step-edge are likely to get oxidized, and the oxidized step-edge turns out to be a catalytic reaction center for CO oxidation. The increase in temperatures and p_{CO}/p_{O_2} ratios promotes the coverage of *CO at the active $Cu^{\delta+}$ sites. Accordingly, the reaction mechanism varies from the LH mechanism to the M-vK mechanism. Our results also highlight the importance of modeling more realistic reaction condition in

providing valid mechanistic understanding of catalyst behaviors. The reaction mechanism and active centers strongly depend on the surface composition of the catalyst, which can be varied by changing the reaction conditions. Under the experimental condition of CO oxidation on CuTiO_x/Cu(111) applied previously,⁷ the active Cu^{δ+} sites are mostly occupied by O₂ and the coverage of *CO is only about 30% (Figure 3). In another word, the CuTiO_x/Cu(111) step edge is likely dominated by *O₂-occupied sites, which leads to the surface oxidation and the promotion of CO to CO₂ conversion via the LH mechanism. In contrast, the contribution for *CO-occupied sites via the M-vK mechanism is much less, which is about 10% of overall activity.

Catalysis by single atomic center would be the most efficient class of heterogeneous catalysis, CO oxidation for instance,^{28, 29} but such single atomic center should be inevitably volatile upon the repeating reaction. Our mixed-oxide framework provides structural robustness to such single Cu⁺ reaction center by evenly embedding Cu⁺ ions in a TiO_x matrix. Such structural motif is more stable than that of Cu_xO under the CO oxidation condition. Unfortunately, on the CuTiO_x/Cu(111) terrace the single Cu⁺ site isolated from each other is not active. The reaction requires the synergy among the Cu^{δ+} sites, Ti^{δ+} sites and Cu(111) at the step edge. In this case, the ensemble effect due to the presence of both Cu^{δ+} sites and Ti^{δ+} sites promotes the reaction. O₂ adsorption and dissociation is facilitated by either cooperation between Cu^{δ+} and Ti^{δ+} sites or Ti^{δ+} sites alone, while the stability of *CO at the Cu^{δ+} sites still remains. In addition, the strong CuTiO_x-Cu(111) interaction (electronic effect) leads to the reduction of Ti^{δ+} ions at the interface and therefore the enhances activity toward O₂. Finally, although the single site catalysis does not work for CO oxidation on CuTiO_x/Cu(111), the idea of isolation and stabilization of single catalytic center can be intensively considered for rational design of oxide

based catalysts. In this aspect, mixed-oxides like CuTiO_x can be classified as a new kind of heterogeneous catalyst to achieve the stabilization, homogeneous distribution, and the chemical modification of atomic sized reaction center.

5. Conclusions

Here we employed DFT to provide fundamental understanding to the experimentally observed activity and stability of model $\text{CuTiO}_x/\text{Cu}(111)$ catalyst toward CO oxidation. The unique structural feature of CuTiO_x allows the single Cu^+ centers on the terrace evenly separated from each other by the TiO_x matrix. Such motif is able to enhance the stability of Cu_xO under the reaction condition. However, the isolated single site of Cu^+ on the terrace is not able to catalyze CO oxidation. The reaction via the LH mechanism is prevented due to the selective adsorption Cu^+ sites to CO rather than O_2 , and that via the M-vK mechanism is hindered due to the high stability of the mixed oxide.

The active site for CO oxidation is the step-edge of $\text{CuTiO}_x/\text{Cu}(111)$. The synergy among Cu^+ ions, TiO_x matrix and $\text{Cu}(111)$ is the key for the conversion of CO to CO_2 on $\text{CuTiO}_x/\text{Cu}(111)$, where all of them contribute to the reaction via electronic and/or ensemble effects. In this case, both $\text{Cu}^{\delta+}-\text{Ti}^{\delta+}$ and $\text{Ti}^{\delta+}-\text{Ti}^{\delta+}$ bridge sites are able to stabilize O_2 and break O-O bond efficiently during CO oxidation, while $\text{Cu}^{\delta+}$ still binds CO. $\text{Cu}(111)$ also participate in the reaction to reduce the $\text{Ti}^{\delta+}$ ions at the interface, which enhances the activity toward O_2 . Depending on the reaction conditions, the coverages of $^*\text{O}_2$ and $^*\text{CO}$ at the active $\text{Cu}^{\delta+}$ sites are affected, which determines the dominant mechanism for the CO oxidation to proceed well. The increase in temperatures and $p_{\text{CO}}/p_{\text{O}_2}$ ratios promotes the coverage of $^*\text{CO}$ at the active $\text{Cu}^{\delta+}$ sites, and accordingly, the reaction mechanism varies from the LH mechanism to the M-vK

mechanism. That is, modeling more realistic reaction condition is important to provide valid mechanistic understanding of catalyst behaviors. The reaction mechanism and active centers strongly depend on the surface composition of the catalyst, which can be varied by changing the reaction conditions.

Acknowledgements

Funds for research work were provided by the U.S. Department of Energy, Office of Basic Energy Sciences, under Contract No. DE-SC-00112704. DFT calculations were performed using computational resources at the Center for Functional Nanomaterials, a user facility at Brookhaven National Laboratory, and at the National Energy Research Scientific Computing Center (NERSC), the latter of which is supported by the Office of Science of the U.S. DOE under Contract No. DE-AC02-05CH11231. H.Y.K thank to the support from Basic Science Research Program through the National Research Foundation of Korea (NRF) funded by the Ministry of Education (NRF-2014R1A1A2057335) and internal research fund from Chungnam National University.

Supporting Information. Description of method to estimate the coverage effect; Configurations and energetics for the formation of CO-O type intermediate on the CuTiO_x/Cu(111) terrace during the CO oxidation via the M-vK mechanism. This material is available free of charge via the Internet at <http://pubs.acs.org> .

Reference

1. Stacchiola, D. J.; Senanayake, S. D.; Liu, P.; Rodriguez, J. A., Fundamental Studies of Well-Defined Surfaces of Mixed-Metal Oxides: Special Properties of $\text{Mo}_x/\text{TiO}_2(110)$ {M = V, Ru, Ce, or W}, *Chem. Rev.* **2013**, *113*, 4373-4390.
2. Rodriguez, J. A.; Senanayake, S. D.; Stacchiola, D.; Liu, P.; Hrbek, J., The Activation of Gold and the Water–Gas Shift Reaction: Insights from Studies with Model Catalysts, *Acc. Chem. Res.* **2014**, *47*, 773-782.
3. Bruix, A.; Rodriguez, J. A.; Ramírez, P. J.; Senanayake, S. D.; Evans, J.; Park, J. B.; Stacchiola, D.; Liu, P.; Hrbek, J.; Illas, F., A New Type of Strong Metal–Support Interaction and the Production of H_2 through the Transformation of Water on $\text{Pt}/\text{CeO}_2(111)$ and $\text{Pt}/\text{CeO}_x/\text{TiO}_2(110)$ Catalysts, *J. Am. Chem. Soc.* **2012**, *134*, 8968-8974.
4. Park, J. B.; Graciani, J.; Evans, J.; Stacchiola, D.; Senanayake, S. D.; Barrio, L.; Liu, P.; Sanz, J. F.; Hrbek, J.; Rodriguez, J. A., Gold, Copper, and Platinum Nanoparticles Dispersed on $\text{CeO}_x/\text{TiO}_2(110)$ Surfaces: High Water-Gas Shift Activity and the Nature of the Mixed-Metal Oxide at the Nanometer Level, *J. Am. Chem. Soc.* **2010**, *132*, 356-363.
5. Johnston-Peck, A. C.; Senanayake, S. D.; Plata, J. J.; Kundu, S.; Xu, W.; Barrio, L.; Graciani, J.; Sanz, J. F.; Navarro, R. M.; Fierro, J. L. G.; et al., Nature of the Mixed-Oxide

Interface in Ceria–Titania Catalysts: Clusters, Chains, and Nanoparticles, *J. Phys. Chem. C* **2013**, *117*, 14463-14471.

6. Luo, S.; Nguyen-Phan, T.-D.; Johnston-Peck, A. C.; Barrio, L.; Sallis, S.; Arena, D. A.; Kundu, S.; Xu, W.; Piper, L. F. J.; Stach, E. A.; et al., Hierarchical Heterogeneity at the CeO_x–TiO₂ Interface: Electronic and Geometric Structural Influence on the Photocatalytic Activity of Oxide on Oxide Nanostructures, *J. Phys. Chem. C* **2015**, *119*, 2669-2679.

7. Baber, A. E.; Yang, X.; Kim, H. Y.; Mudiyansele, K.; Soldemo, M.; Weissenrieder, J.; Senanayake, S. D.; Al-Mahboob, A.; Sadowski, J. T.; Evans, J., Stabilization of Catalytically Active Cu⁺ Surface Sites on Titanium–Copper Mixed-Oxide Films, *Angew. Chem. Int. Ed.* **2014**, *53*, 5336-5340.

8. McFarland, E. W.; Metiu, H., Catalysis by Doped Oxides, *Chem. Rev.* **2013**, *113*, 4391-4427.

9. Kim, H. Y.; Lee, H. M.; Pala, R. G. S.; Shapovalov, V.; Metiu, H., Co Oxidation by Rutile TiO₂ (110) Doped with V, W, Cr, Mo, and Mn, *J. Phys. Chem. C* **2008**, *112*, 12398-12408.

10. Ganduglia-Pirovano, M. V.; Popa, C.; Sauer, J.; Abbott, H.; Uhl, A.; Baron, M.; Stacchiola, D.; Bondarchuk, O.; Shaikhutdinov, S.; Freund, H.-J., Role of Ceria in Oxidative Dehydrogenation on Supported Vanadia Catalysts, *J. Am. Chem. Soc.* **2010**, *132*, 2345-2349.

11. Kim, H. Y.; Lee, H. M.; Metiu, H., Oxidative Dehydrogenation of Methanol to Formaldehyde by a Vanadium Oxide Cluster Supported on Rutile TiO₂ (110): Which Oxygen Is Involved?, *J. Phys. Chem. C* **2010**, *114*, 13736-13738.

12. Kim, H. Y.; Lee, H. M.; Pala, R. G. S.; Metiu, H., Oxidative Dehydrogenation of Methanol to Formaldehyde by Isolated Vanadium, Molybdenum, and Chromium Oxide Clusters Supported on Rutile TiO₂ (110), *J. Phys. Chem. C* **2009**, *113*, 16083-16093.
13. Kim, H. Y.; Liu, P., Tuning the Catalytic Selectivity of Copper Using TiO₂: Water-Gas Shift Versus CO Oxidation, *ChemCatChem* **2013**, *5*, 3673-3679.
14. Graciani, J.; Mudiyansele, K.; Xu, F.; Baber, A. E.; Evans, J.; Senanayake, S. D.; Stacchiola, D. J.; Liu, P.; Hrbek, J.; Sanz, J. F.; et al., Highly Active Copper-Ceria and Copper-Ceria-Titania Catalysts for Methanol Synthesis from CO₂, *Science* **2014**, *345*, 546-550.
15. Senanayake, S. D.; Stacchiola, D.; Rodriguez, J. A., Unique Properties of Ceria Nanoparticles Supported on Metals: Novel Inverse Ceria/Copper Catalysts for CO Oxidation and the Water-Gas Shift Reaction, *Acc. Chem. Res.* **2013**, *46*, 1702-1711.
16. Senanayake, S. D.; Mudiyansele, K.; Bruix, A.; Agnoli, S.; Hrbek, J.; Stacchiola, D.; Rodriguez, J. A., The Unique Properties of the Oxide-Metal Interface: Reaction of Ethanol on an Inverse Model CeO_x-Au(111) Catalyst, *J. Phys. Chem. C* **2014**, *118*, 25057-25064.
17. Mudiyansele, K.; Senanayake, S. D.; Feria, L.; Kundu, S.; Baber, A. E.; Graciani, J.; Vidal, A. B.; Agnoli, S.; Evans, J.; Chang, R., et al., Importance of the Metal-Oxide Interface in Catalysis: In Situ Studies of the Water-Gas Shift Reaction by Ambient-Pressure X-Ray Photoelectron Spectroscopy, *Angew. Chem. Int. Ed.* **2013**, *52*, 5101-5105.
18. Royer, S.; Duprez, D., Catalytic Oxidation of Carbon Monoxide over Transition Metal Oxides, *ChemCatChem* **2011**, *3*, 24-65.
19. Jernigan, G. G.; Somorjai, G. A., Carbon-Monoxide Oxidation over 3 Different Oxidation-States of Copper - Metallic Copper, Copper (I) Oxide, and Copper (II) Oxide - a Surface Science and Kinetic-Study, *J. Catal.* **1994**, *147*, 567-577.

20. Baber, A.; Xu, F.; Dvorak, F.; Mudiyansele, K.; Soldemo, M.; Weissenrieder, J.; Senanayake, S.; Sadowski, J.; Rodriguez, J.; Matolin, V.; et al., In Situ Imaging of Cu₂O under Reducing Conditions: Formation of Metallic Fronts by Mass Transfer, *J. Am. Chem. Soc.* **2013**, *135*, 16781-16784.
21. Huang, T. J.; Tsai, D. H., CO Oxidation Behavior of Copper and Copper Oxides, *Catal. Lett.* **2003**, *87*, 173-178.
22. Kresse, G.; Furthmüller, J., Efficient Iterative Schemes for Ab Initio Total-Energy Calculations Using a Plane-Wave Basis Set, *Phys. Rev. B* **1996**, *54*, 11169-11186.
23. Perdew, J. P.; Burke, K.; Ernzerhof, M., Generalized Gradient Approximation Made Simple, *Phys. Rev. Lett.* **1996**, *77*, 3865-3868.
24. Blochl, P. E., Projector Augmented-Wave Method, *Phys. Rev. B* **1994**, *50*, 17953.
25. Dudarev, S. L.; Botton, G. A.; Savrasov, S. Y.; Humphreys, C. J.; Sutton, A. P., Electron-Energy-Loss Spectra and the Structural Stability of Nickel Oxide: An LSDA+U Study, *Phys. Rev. B* **1998**, *57*, 1505-1509.
26. Liu, P., Water-Gas Shift Reaction on Oxide/Cu(111): Rational Catalyst Screening from Density Functional Theory, *J. Chem. Phys.* **2010**, *133*, 204705-204707.
27. Vidal, A. B.; Liu, P., Density Functional Study of Water-Gas Shift Reaction on M₃O_{3x}/Cu(111), *Phys. Chem. Chem. Phys.* **2012**, *14*, 16626-16632.
28. An, W.; Baber, A. E.; Xu, F.; Soldemo, M.; Weissenrieder, J.; Stacchiola, D.; Liu, P., Mechanistic Study of CO Titration on Cu_xO/Cu(1 1 1) (X≤2) Surfaces, *ChemCatChem* **2014**, *6*, 2364-2372.

29. Falsig, H.; Hvolbæk, B.; Kristensen, I. S.; Jiang, T.; Bligaard, T.; Christensen, C. H.; Nørskov, J. K., Trends in the Catalytic CO Oxidation Activity of Nanoparticles, *Angew. Chem. Int. Ed.* **2008**, *47*, 4835-4839.

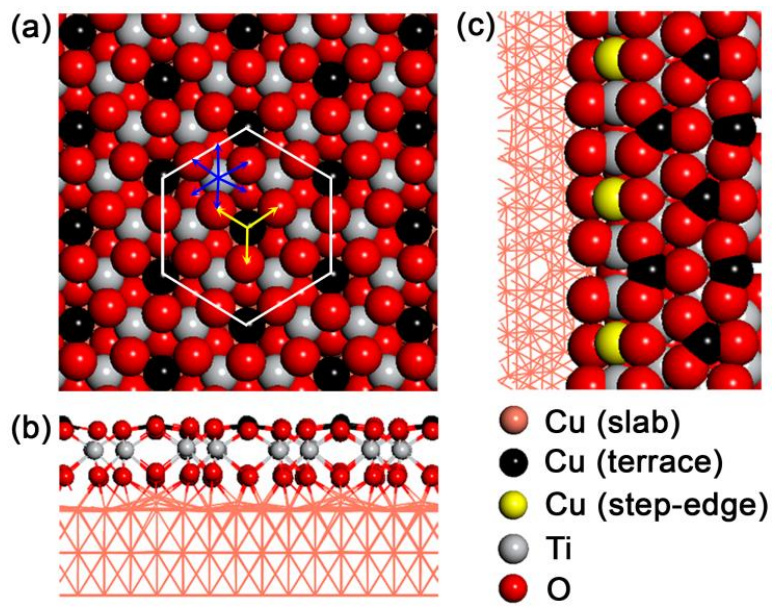


Figure 1. Morphology of CuTiO_x/Cu(111) model catalysts (a) Top and (b) side views of terrace. A representative structural motif is highlighted by white hexagon including six-coordinated Ti ions (blue arrows) and three-coordinated Cu ion (yellow arrows). (c) Top view of step edge.

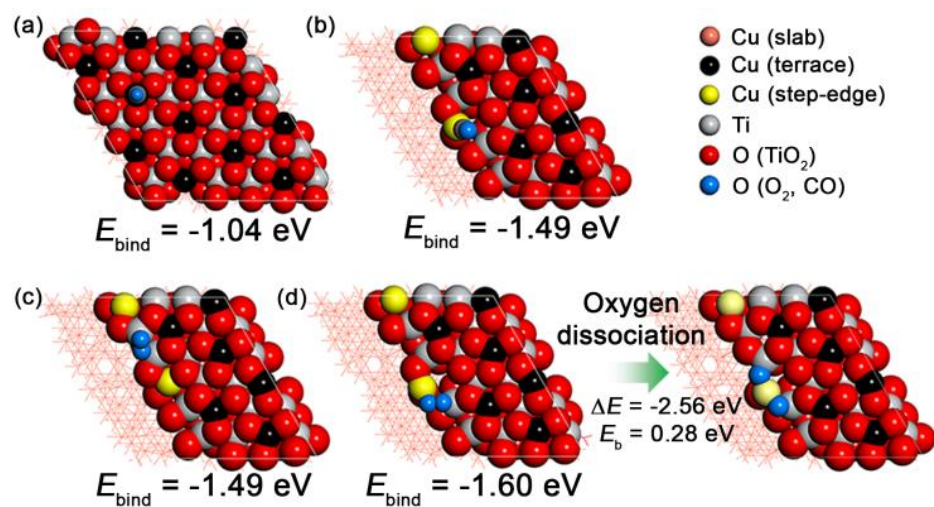


Figure 2. Available adsorption geometries and energetics of reacting molecules (CO and O₂) on the catalyst surface (a): terrace and (b)~(d): step-edge. The E_{bind} of O₂ on the terrace Cu ion is positive (0.203 eV, not shown for brevity). This confirms the strong CO preference of the terrace Cu ions.

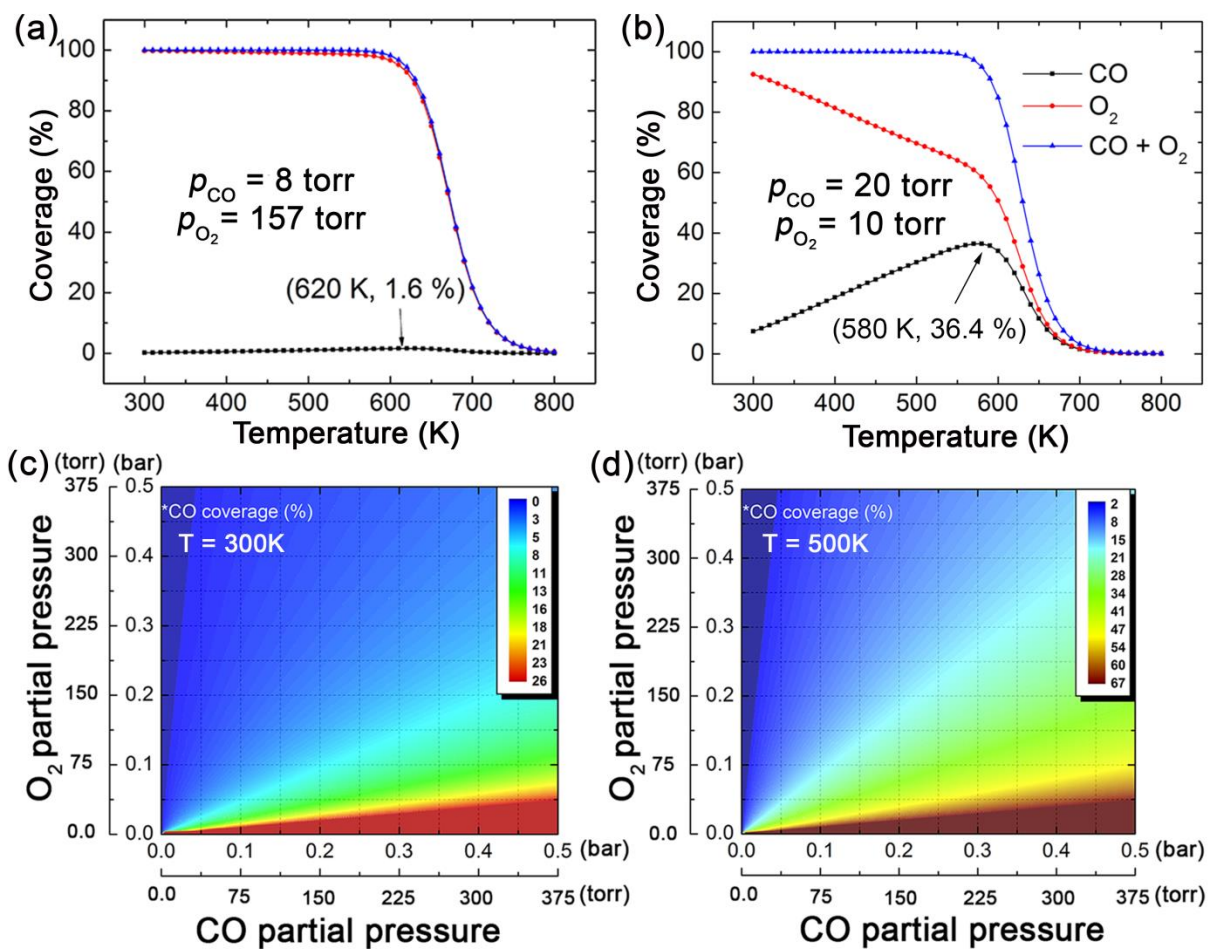


Figure 3. Calculated relative coverage of $*\text{CO}$ and $*\text{O}_2$ at the $\text{Cu}^{\delta+}$ sites on the terrace of $\text{CuTiO}_x/\text{Cu}(111)$ as a function of temperature under O_2 -rich (a) and CO -rich (b) conditions. Calculated relative coverage of $*\text{CO}$ as a function of partial pressure of CO and O_2 at 300 K (c), and 500 K (d).

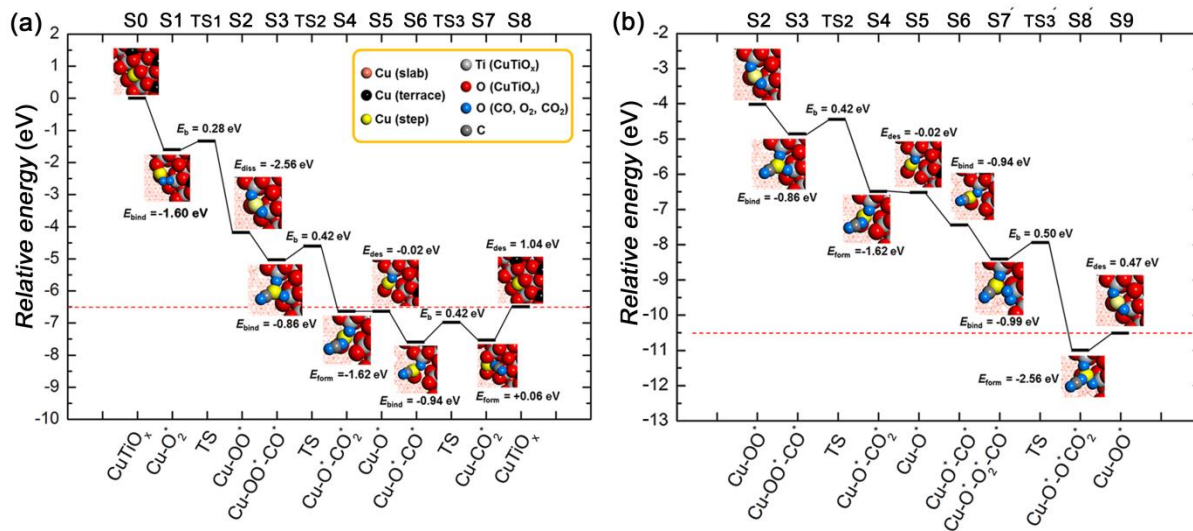


Figure 4. DFT-optimized pathways of the CO oxidation catalyzed by the CuTiO_x/Cu(111) step-edge, which is preferentially adsorbed by O₂ at the Cu^{δ+} sites (a), where the alternative path for the oxidation of the second CO is shown in (b). The red-dotted line represents the total energy released upon the oxidation of two CO molecules (6.51 eV). The notation S_x and TS_x represent the xth stage of the reaction intermediate and the xth transition state, respectively.

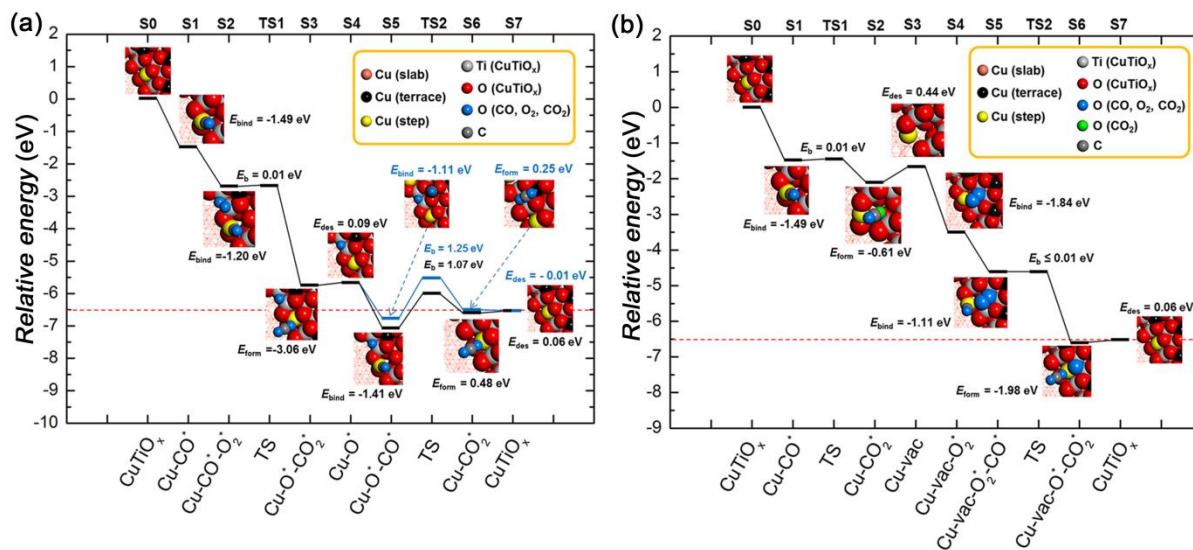


Figure 5. DFT-optimized pathways of the CO oxidation catalyzed by the CuTiO_x/Cu(111) step-edge, which is preferentially adsorbed by CO at the Cu^{δ+} sites: (a) Reaction via the LH mechanism; (b) Reaction via the M-vk mechanism. The red-dotted line represents the total energy released upon the oxidation of two CO molecules (6.51 eV). The notation S_x and TS_x represent the xth stage of the reaction intermediate and the xth transition state, respectively.

TOC graphic

